Projection Based Real-time Material Appearance Manipulation

Toshiyuki Amano
Faculty of Systems Engineering, Wakayama University
amano@sys.wakayama-u.ac.jp

Abstract

We introduce a new projection display technique that converts a visual material appearance of target object. Unlike conventional projection display, our approach allowed us successive material appearance manipulation by the projector camera feedback without scene modeling. First, we introduce an appearance control framework with a coaxial projector camera system. Next, we introduce two image based material appearance manipulation methods of translucency and glossiness. Last, we verify the ability of the material appearance manipulation of the proposed display technique through the experiments.

1. Introduction

The material perception from the human vision system depends on only its appearance, and the appearance can be influenced by not only own reflection characteristics but also environmental illumination. Therefore, precisely designed illumination projection can give the human material perception different on the same object's surface property.

There are several studies on the projection display technique which alternate visual appearance on the object's surface. Pioneering work of the projection based material appearance manipulation, Raskar et al. proposed the Shader Lamps that can represent virtual texture and animate shading on the physical model [16]. Mukaigawa et al. [13] proposed a Virtual Photometric Environment system which enables us to arbitrarily control lighting directions and reflection properties of objects. For the projection display, the employment of BRDF for the optical property model enabled the high quality material representation. Besides, a high quality projection display technique with accurate modeling was proposed [15]. Combined structure light projection that employed photometric stereo and surface normal smoothing obtained a high accurate 3D model.

The another trend in projection display is the overlay projection. Above mentioned works regard a projection surface as white and non textured surface, but Aliga et al. applied overlay projection on a degenerated ancient base for virtual restoration [1], and proposed an appearance editing system [10]. Shimazu et al. employed the textured object which made by 3D printer or Rapid Prototyping for 3D high dynamic range (HDR) display system [17]. The overlay projection on the textured object boosts its contrast and shows us a HDR appearance on the object by precisely calculated projection. Its capability is not limited for virtual restoration, appearance editing and HDR display and suggests it can apply for the material appearance manipulation in same framework.

Many applications for material appearance manipulation are expected in psychological experiment, scientific simulation, product design, digital signage, entertainment systems and human vision support, etc. Since not all assumed users are specialist of projector camera system, the ease of use comparable to a conventional lighting system is required for the popularization of this technique. However, existing approaches require a pre-measuring of object's shape and registration. Both procedures are not easy for end user. In addition, conventional approach cannot apply for the dynamic scene. For this reason, we employed an appearance control technique for the dynamic reflection estimation and an image based material appearance manipulations, and we aimed to the successive material appearance manipulation of the object in the real world without physical modeling.

2. Adaptive Photometric Compensation

Since most of above projection display techniques estimate surface reflection from a pre-measured shape with proper Lambert reflection approximation, a physically correct appearance editing can be applied. However, not only the modeling of shape and reflectance but also accurate registration and precise ambient lighting setting are required. These requirements are not difficult for the completely designed booth such as theme parks and museums, but are not easy for daily environment, and the image-based approach used a projector camera feedback can be a good solution.

In the pioneering works of the projector camera system, Nayar et al. proposed the radiometric compensation for the non-uniform textured screen with projector camera feedback [14]. Grossberg et al. considered the ambient light

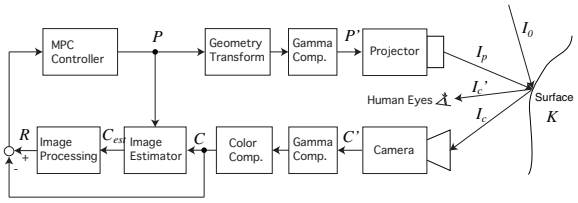

Figure 1. Appearance control by the model predictive control.

term for the photometric model and they showed the ability to alternate the appearance of 3D textured object [9]. A similar modeling is also proposed by Yoshida et al. for projection based virtual restoration of damaged oil painting [18]. In the later work, Fujii et al. [8] applied this radiometric compensation technique in dynamic scene with coaxial device configuration. The radiometric compensation was also implemented with smart calibration [5], and it was also attempted from the view of the human visual perception [3].

Different to radiometric compensation, the appearance control techniques can enhance, change, and replace the visible appearance according to the original appearance. The superimposed dynamic range technique accomplished a high dynamic range display and a color compensation on the printed media by the illumination projection [6]. Furthermore, the projector camera feedback framework enabled not only appearance enhancement, but also, appearance control successively [2].

3. Projector Camera System

This section explains our successive material appearance manipulation method that used the projector camera system. First, we introduce an appearance control framework. Second, we show our coaxial projector camera system for dynamic adaptation. Third, we consider the inverse square law of projection illuminance, and derive the conditions for appearance control framework application to the non planar projection-target placed at different depth.

3.1. Appearance Control Framework

Amano et al. proposed an appearance control technique with projector camera feedback [2]. This framework shown in figure 1 enabled a desired appearance manipulation with model predictive control by the illumination projection. We employ this framework with several modifications.

In the diagram, all properties have three color components of R, G and B channels, and now we consider a single pixel relation. The environment illumination $I_0 \in \mathcal{R}^3$ and projected illumination $I_p \in \mathcal{R}^3$ are mixed and reflected on the surface $K \in \mathcal{R}^{3\times3} = diag(k_R, k_G, k_B)$. Then, the camera capture reflected light ray

$$I_c = K(I_p + I_0). \tag{1}$$

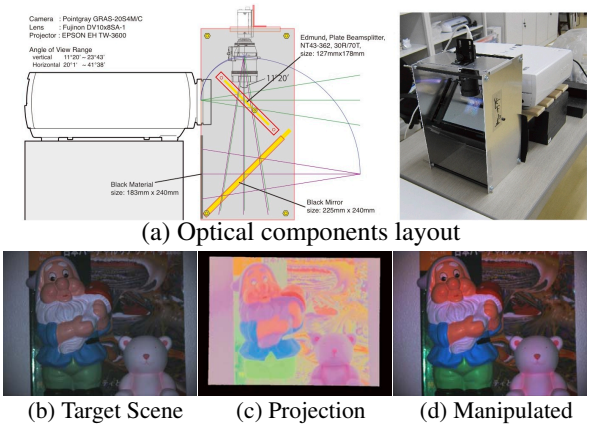

(a) Optical components layout

(b) Target Scene (c) Projection (d) Manipulated

Figure 2. A coaxial projector camera system.

After the color and gamma correction, a compensated image C is obtained. However, this color compensation means the system uses a projector's color space and it makes a perceptual difference with an actual scene view. This error might be small, but, it is critical when we try to show an accurate color of post image processing result onto the projection target. Hence, we apply this color conversion to projection image P. Then, an estimated relative physical surface reflectance can be written as

$$\hat{K} = diag\{C./(MP + C_0)\} \tag{2}$$

by using P and C. Where C_0 is an image captured under minimum power (turn off) projections, M is a color mixing matrix which can be obtained by conventional calibration procedure as shown in [14, 9]. The operator $./$ means component-wise division. From eq. 2, we can obtain an underlaying appearance which means a captured image under the white illumination

$$C_{est} = \hat{K} C_{white}, \tag{3}$$

where $C_{white} = (1, 1, 1)^T$. The projection image P is controlled by the MPC Controller which based on model predictive control theory, then I_P is projected after Geometrical Transform and Gamma Compensation of P.

3.2. Coaxial Projector Projection System

The coaxial projector camera setting (More precisely, co-placed entrance pupils optics) ensure an invariant pixel map and enable the projector camera feedback on the arbitrary shape object without any individualized calibration.

Figure 2(a) shows our system configuration. The system has a beam splitter to optically place both entrance pupils in the same place, and it separates outgoing and incoming light rays. Major concern for this optical layout is the directly come scattered-projection light of cases' inside makes an artificial misty image then it causes an image quality drop.

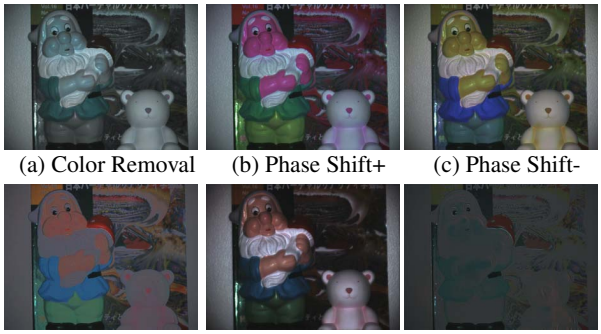

(a) Color Removal (b) Phase Shift+ (c) Phase Shift-

(d) Brightness EQ (e) Contrast Boost (f) Optical Hiding

Figure 3. Various results of appearance control.

For this solution, our system employed a light absorbing blackout material with a black mirror reflection. Since the entrance pupils are co-aligned, we get a projection pattern (c) of a same aspect as (b) in figure.With the overlay projection by this pattern, we can enhance the scene color saturation as shown by (d).

Other appearance control results shown in figure 3 were obtained with the image processing algorithms of (a) grayscale conversion, (b-c) color phase shift, (d) brightness equalization, (e) power function operation, and (f) paint over R with solid gray color.

3.3. Inverse Square Law of Illuminance

As shown in equation 2, the physical surface reflection is estimated from component wise division of C by an expected image brightness of projected image onto the white calibration target $MP + C_0$. However, its overall flux of light in the unit area changes with distance d from a projector based on the inverse square law. Thus, the d makes an influence on the reflection estimation

$$\hat{K}(d) = \left\{ \frac{{d_0}^2}{d^2} + \left(1 - \frac{{d_0}^2}{d^2}\right) \frac{I_0}{I_p + I_0} \right\} \hat{K}(d_0). \quad (4)$$

Where d_0 is a distance to the calibration plane. This equation suggests, apparent reflection ratio follows the inverse square law when $I_0 \ll I_p$, and correct appearance control can operate on the solid object with a proper gain of R if the working-distance of projection target is much less than d. In this research, we assume these conditions.

4. Image Based Visual Material Conversion

4.1. Translucent Perception

Recently, the study on the human material perception has attracted attention. Motoyoshi studied on the human discrimination capability of the translucent materials and he showed the idea that the contrast and sharpness of the nonspecular image component have a strong impact on the

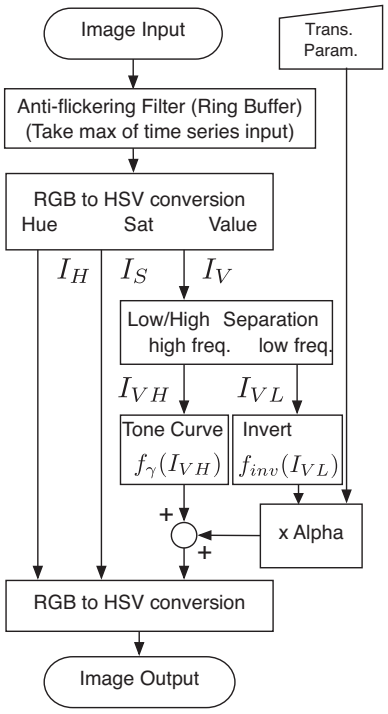

Figure 4. Processing flow of the translucency manipulation.

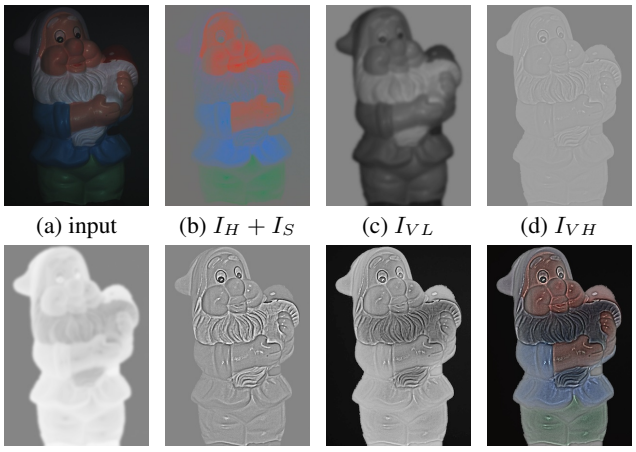

(a) input (b) $I_H + I_S$ (c) I_{VL} (d) I_{VH}

(e) $f_{inv}(I_{VL})$ (f) $f_\gamma(I_{VH})$ (g)$f_{inv} + f_\gamma$ (h) output

Figure 5. Detailed process of translucency manipulation.

judgment of translucency [11]. His study showed an image reconstruction that used an inverse tone mapping of low spatial frequency component can make the appearance of the opaque object look translucent. We inherits this idea and implemented an image based visible translucent manipulation algorithm as shown by figure 4.

The original study on translucency perception applied for grayscale image. However, most of target which we want to apply has color. Therefore, we apply HSV sepa-

ration to (a) the input image at the beginning as shown in the figure 5. Then, we apply spatial frequency filter to the value component I_V and we get (c) a low frequency component I_{VL} and (d) a high frequency component I_{VH}. Next, we apply inverse tone mapping

$$f_{inv}(x) = 1 - x \tag{5}$$

for (e) I_{VH}. This mapping makes a similar brightness distribution produced by the refracted rays. For I_{VH}, we apply tone curve

$$f_\gamma(x) = x^{\gamma_t} \tag{6}$$

to enhance specular reflection on the object. Where γ_t is a specular gain. Last, translucent conversion (g) is calculated by the mixing of $f_{inv}(\cdot)$ and $f_\gamma(\cdot)$ with ratio α, and we get a color output by merging with I_H and I_S, after the addition of $min(I_{VL})$. This image processing is applied to C_{est} and the output gives a reference image R in the figure 1.

4.2. Glossiness Perception

Motoyoshi et al. also have shown that the skewness of luminance histogram and the skewness of sub-band filter output are correlated with a surface glossy and inversely correlated with diffuse reflectance [12]. In other words, this study suggests a consecutive tone mapping which produces a positive-skewed histogram converts a matt object's appearance to glossy. We implement this idea as another material perception manipulation.

For the implementation, we apply this knowledge to the brightness component to manipulate the color scene's glossiness as shown in figure 6 . First, the histogram equalization is applied to the value component I_V and we get I_{VHE} as shown in figure 7 (a), (b). Then, we applied histogram equalization before tone mapping of

$$f_{skew}(x) = (1 - \beta)x^{\gamma_g} + \beta. \tag{7}$$

Where, γ_g is a skewness parameter, β is a offset of image brightness. With the histogram equation, this tone mapping assure a positive skewness of histogram which is proportional to

$$p(y) = \begin{cases} 0 & (y < \beta) \\ \frac{1}{\gamma_g(1-\beta)^{1/\gamma_g}}(y-\beta)^{\frac{1-\gamma_g}{\gamma_g}} & otherwise \end{cases} \tag{8}$$

in the processed image statistically and the skewness and brightness offset are controlled by β, γ_g. Then, we merge down $f_{skew}(I_{VHE})$ with I_H, I_S and get output image.

5. Implementation Results and Discussions

Our projector camera system shown in figure 2 consist of 1600 × 1200 pixels IEEE1394 camera, 1920 × 1080 pixels 3 LCD projector. The Gamma value of the camera is adjustable by the hardware configuration and we set it linear.

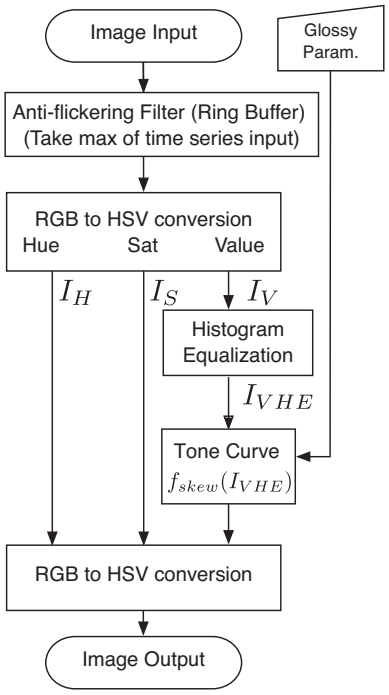

Figure 6. Processing flow of the glossiness manipulation.

(a) I_V (b) I_{VLHE} (c) f_{skew} (d) output

Figure 7. Detailed process of glossiness manipulation.

Thus, we can skip gamma compensation to get C. Next, we applied linearization of the projection illumination and we obtained a color mixing matrix by conventional calibration. We used OpenMP with the Xeon based multi core hardware (12 Core Mac Pro, 2.4 GHz) and achieved up to 8 frames processing per second.

The figure 8 shows four target samples placed in front of a black stage background. Each object made with (a) cray (left : dwarf - with gloss finish, right : bear - without gloss finish), (b) plastic (toy figure), (c) silk (necktie) respectively. All experiments used this projector camera system in the indoor environment that has fluorescent ceiling lights. Scene illuminance without projection was 350 lux and with full white illumination projection was 3930 lux. This condition satisfies $I_0 \ll I_p$, and working-distance is enough short because the projector has a limited depth of focus.

(a) clay (b) plastic (c) silk

Figure 8. Four target samples.

$\alpha = 0.2$ $\alpha = 0.4$ $\alpha = 0.6$ $\alpha = 0.8$

Figure 9. Processing results of translucency manipulation.

5.1. Translucent Manipulation

We implemented an image processing algorithm shown in figure 4 in the appearance control framework. First, we manually adjusted projection gain of R which gives proper illumination of I_P (not saturated, but not too dark), then we got the results for various translucency manipulation parameter of α as shown in figure 9. From left to right, each row shows the translucency manipulation results by the $\alpha = 0.2, 0.4, 0.6, 0.8$, and $\gamma_t = 2.0$ is used.

As shown in figure 9, we can see the low frequency component of scene is inverted and the contour parts of dwarf's body, bears face, etc. became bright along with increment of α. It is completely a different appearance from the original appearance, and its optical feature cannot explain without light emission from our physical experience. From these manipulated appearances, we can suppose that these objects have subsurface scattering because of their translucent objects. However, since the high frequency component cannot be extracted or is not contained naturally, the specular reflections cannot be seen on the manipulation results. In addition, we could not get a translucency perception from the necktie. It is because efficiency of the image based translucent manipulation is strongly depends on the original appearance not only on our knowledge.

5.2. Glossiness Manipulation

Figure 10 shows manipulation results of glossiness manipulation. From left to right, each row shows the result by the $\gamma_g = 3.0, 5.0, 7.0, 9.0$, and $\beta = 0.13$.

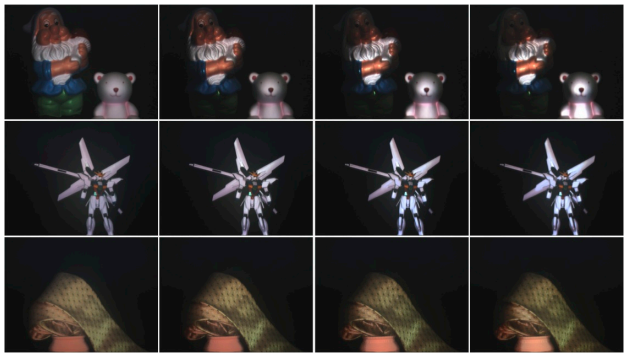

$\gamma_g = 3.0$ $\gamma_g = 5.0$ $\gamma_g = 7.0$ $\gamma_g = 9.0$

Figure 10. Processing results of glossiness manipulation.

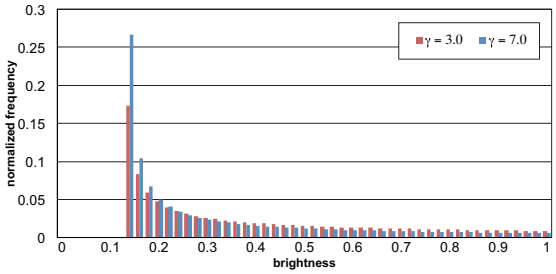

Figure 11. Expected histogram by the glossiness manipulation.

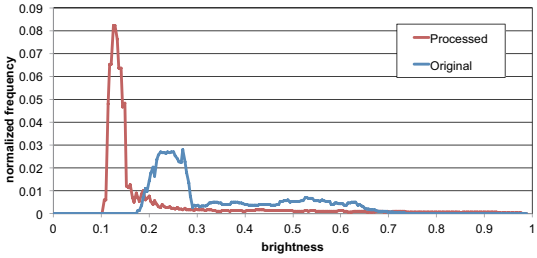

Figure 12. The histogram change by the glossiness manipulation.

Since the brightness on the object can be influenced by albedo, face and body part of dwarf became dark and made an unbalanced appearance (see top row). In contrast, we can confirm more strong shiny reflection along with the increment of γ_g as seen in the bear. As shown in second row, this is efficient not only for a smooth shape object, but also rectilinear shape object. In addition, it is also applicable for the smooth fabric as shown in third row.

Both conversions of the contrast boost shown in figure 3(e) and the glossiness manipulation are based on the power function and show similar processing results. However, unlike naive power conversion, the glossiness manipulation process employed a histogram-equalization, and it ensure a designed histogram distribution as shown in figure 11 on the manipulation result. Normalized frequency (vertical axis) of each bin is exponentially reduced along

with increment of the brightness (horizontal axis). The brightness offset and skewness of the histogram are adjustable with β and γ_g. Figure 12 shows the histograms of original appearance (figure 8(a)) and a manipulation result (top row, $\gamma_g = 7.0$ in figure 10) shown by a blue line and a red line respectively. Obviously, we can see the histogram has been modified to the designed distribution in the real world. Since the mechanism of material perception is currently being intensively investigated, the optimal shape is less well understood, but, we can apply the histogram specification algorithm [7] once we have a detailed distribution.

5.3. Pseudo Specular Reflection Addition

The lack of specular reflection inhibits us clear translucent perception. However, not all images of projection targets contain specular reflection. Thus, we have to add some pseudo specular reflection which related surface shape.

Fortunately, we can assume a single light source situation under the $I_0 \ll I_p$ condition and the light direction is given. Hence, it is easy to estimate the surface normal from the gradient of C_{set} for each segmented color region. For the other method, we can use simultaneous estimation method of an albedo and a shape [4].

6. Conclusion

It is not hard the material appearance manipulation can be widely accepted for a display technique in many fields. One of key factor for popularization is its ease of use, and we proposed adaptive manipulation technique that not required individual calibration. For the first attempt, we implemented material appearance manipulation of translucency and glossiness. However, the specular reflections could not be seen on the translucency manipulation results. Its lack inhibits a clear translucent perception such as when we see a polished clear glass.

In the future work, we attempt pseudo specular reflection addition for the translucent manipulation. Then, we will evaluate our technique through user study. Next, we are going to develop other material appearance manipulation of metallic, wetness, warm and cold.

Acknowledgement

This work was supported by MEXT KAKENHI Grant Number 23135523, 25135723.

References

[1] D. G. Aliaga, A. J. Law, and Y. H. Yeung. A virtual restoration stage for real-world objects. *ACM Trans. Graph.*, 27(5):149:1–149:10, Dec. 2008. 1

[2] T. Amano and H. Kato. Appearance control using projection with model predictive control. In *Proc. of ICPR*, pages 2832–2835. IEEE Computer Society, 2010. 2

[3] M. Ashdown, T. Okabe, I. Sato, and Y. Sato. Robust content-dependent photometric projector compensation. In *Proc. of the 2006 Conference on CVPR Workshop*, pages 60–67. IEEE Computer Society, 2006. 2

[4] J. T. Barron and J. Malik. High-frequency shape and albedo from shading using natural image statistics. volume 9, pages 2521–2528. IEEE, 2011. 6

[5] O. Bimber, A. Emmerling, and T. Klemmer. Embedded entertainment with smart projectors. *Computer*, 38:48–55, 2005. 2

[6] O. Bimber and D. Iwai. Superimposing dynamic range. *ACM Trans. Graph.*, 27(5):150:1–150:8, Dec. 2008. 2

[7] D. Coltuc, P. Bolon, and J.-M. Chassery. Exact histogram specification. *Image Processing, IEEE Transactions on*, 15(5):1143–1152, May. 6

[8] K. Fujii, M. D. Grossberg, and S. K. Nayar. A projector-camera system with real-time photometric adaptation for dynamic environments. In *Proc. of the CVPR*, volume 2, page 1180, 2005. 2

[9] M. D. Grossberg, H. Peri, S. K. Nayar, and P. N. Belhumeur. Making one object look like another: Controlling appearance using a projector-camera system. In *Proc. IEEE Conf. Computer Vision and Pattern Recognition*, volume 1, pages 452–459, 2004. 2

[10] A. J. Law, D. G. Aliaga, B. Sajadi, A. Majumder, and Z. Pizlo. Perceptually based appearance modification for compliant appearance editing. *Computer Graphics Forum*, 30(8):2288–2300, 2011. 1

[11] I. Motoyoshi. Highlight-shading relationship as a cue for the perception of translucent and transparent materials. *J Vis*, 10(9):6, 2010. 3

[12] I. Motoyoshi, S. Nishida, L. Sharan, and E. H. Adelson. Image statistics and the perception of surface qualities. *Nature*, 447:206–209, Apr. 2007. 4

[13] Y. Mukaigawa, M. Nishiyama, and T. Shakunaga. Virtual photometric environment using projector. In *Proceedings of the International Conference on Virtual Systems and Multimedia*, pages 544–553, 2004. 1

[14] S. K. Nayar, H. Peri, M. D. Grossberg, and P. N. Belhumeur. A projection system with radiometric compensation for screen imperfections. In *IEEE International Workshop on Projector-CameraSystems*, 2003. 1, 2

[15] T. Okazaki, T. Okatani, and K. Deguchi. A projector-camera system for high-quality synthesis of virtual reflectance on real object surfaces. *IPSJ Transactions on Computer Vision and Applications*, 2:71–83, 2010. 1

[16] R. Raskar, G. Welch, K.-L. Low, and D. Bandyopadhyay. Shader lamps: Animating real objects with image-based illumination. In *Proc. of the 12th Eurographics Workshop on Rendering Techniques*, pages 89–102, 2001. 1

[17] S. Shimazu, D. Iwai, and K. Sato. 3d high dynamic range display system. In *Proceedings of the 2011 10th IEEE International Symposium on Mixed and Augmented Reality*, ISMAR '11, pages 235–236, 2011. 1

[18] C. H. T. Yoshida and K. Sato. A virtual color reconstruction system for real heritage with light projection. In *Proc. of VSMM*, pages 1–7, 2003. 2